

DUKE-TH-96-126

Chemical Equilibration of an Expanding Quark-Gluon Plasma

Dinesh Kumar Srivastava, Munshi Golam Mustafa

Variable Energy Cyclotron Centre, 1/AF Bidhan Nagar, Calcutta 700 064

Berndt Müller

Department of Physics, Duke University, Durham, North Carolina 27708-0305

(October 4, 2018)

Abstract

The chemical equilibration of the parton distribution in collisions of two heavy nuclei at the CERN Large Hadron Collider is investigated. Initial conditions are obtained from a self-screened parton cascade calculation. The onset of transverse expansion of the system is found to impede the chemical equilibration. The system initially approaches chemical equilibrium, but then is driven away from it, when the transverse velocity becomes large.

PACS: 25.75.Ld, 12.38.Mh

Typeset using REVTeX

It is expected that very highly energetic heavy ion collisions lead to the formation of a new phase of strongly interacting matter, called the quark-gluon plasma (QGP). At collider energies it seems reasonable to visualize the two nuclei as two clouds of valence and sea partons which pass through each other and interact [1]. The multiple parton collisions are thought to produce a dense plasma of quarks and gluons. After its formation this plasma will expand, cool, and become more dilute. If quantum chromodynamics admits a first-order deconfinement or chiral symmetry phase transition, it is likely that the system will pass through a mixed phase of quarks, gluons, and hadrons, before the hadrons lose thermal contact and stream freely towards the detectors.

Several questions about the structure of the matter formed in these nuclear collisions arise. Does the initial partonic system attain kinetic equilibrium? Probably yes, as the initial parton density is large, forcing the partons to suffer many collisions in a very short time [2]. Does it attain chemical equilibration? This will depend on the time available [3–5] to the partonic system before it converts into a mixed phase. The time available for this is perhaps too short (3–5 fm/c) at the energies ($\sqrt{s} \leq 100$ GeV/nucleon) to be reached at the Relativistic Heavy Ion Collider (RHIC). At the energies ($\sqrt{s} \leq 3$ TeV/nucleon) that will be achieved at the CERN Large Hadron Collider (LHC) this time could be large (more than 10 fm/c). If one considered only a longitudinal expansion of the system, the QGP formed at LHC energies would approach chemical equilibrium very closely, due to the higher initial temperature predicted to be attained there. However, the life-time of the plasma would also be large enough to allow a rarefaction wave from the surface of the plasma to approach the center. We shall see that this could have interesting consequences for the evolution of the plasma.

It has recently been shown [6] that color screening provides a mechanism for the elimination of infrared divergences in the partonic cascades following the interaction of two heavy nuclei. Early, hard scatterings produce a medium which screens the longer ranged color fields associated with softer interactions. When two heavy nuclei collide at high enough energy, the screening occurs on a length scale where perturbative QCD still applies. This approach yields predictions for the initial conditions of the forming QGP without the need for cut-off parameters. The resulting values to be adopted in the present study are listed in Table I. They show that the QGP initially is extremely hot, with temperatures around 1 GeV, but not chemically equilibrated.

Once the kinetic equilibrium has been attained we assume that the system can be described by the equation for conservation of energy-momentum of an ideal fluid:

$$\partial_\mu T^{\mu\nu} = 0, \quad T^{\mu\nu} = (\epsilon + P)u^\mu u^\nu + Pg^{\mu\nu} \quad (1)$$

where ϵ is the energy density and P is the pressure measured in the frame comoving with the fluid. We use natural units ($\hbar = c = 1$). The four-velocity vector u^μ for the fluid satisfies the constraint $u^2 = -1$. For a partially equilibrated plasma of massless particles the equation of state can be written as

$$\epsilon = 3P = [a_2\lambda_g + b_2(\lambda_q + \lambda_{\bar{q}})]T^4 \quad (2)$$

where $a_2 = 8\pi^2/15$, $b_2 = 7\pi^2N_f/40$, $N_f \approx 2.5$ is the number of dynamical quark flavors, and λ_k is the fugacity for the parton species k . We take the speed of sound $c_s = 1/\sqrt{3}$ as implied by (2) and solve the hydrodynamic equations (1) for a system undergoing a boost

invariant longitudinal (z -axis) and cylindrically symmetric transverse expansion (see Ref. [7] for details) with initial conditions obtained earlier. It is sufficient to solve the problem for $z = 0$, because of the assumption of boost invariance. Confining ourselves [3] to the dominant reactions $gg \leftrightarrow ggg$, and $gg \leftrightarrow q\bar{q}$ for the equilibration of the partons, we write the master equations governing the parton densities as [3]

$$\begin{aligned}\partial_\mu(n_g u^\mu) &= n_g(R_{2 \rightarrow 3} - R_{3 \rightarrow 2}) - (n_g R_{g \rightarrow q} - n_q R_{q \rightarrow g}) \\ \partial_\mu(n_q u^\mu) &= \partial_\mu(n_{\bar{q}} u^\mu) = n_g R_{g \rightarrow q} - n_q R_{q \rightarrow g},\end{aligned}\quad (3)$$

in an obvious notation. These equations lead to partial differential equations for the fugacities:

$$\begin{aligned}\frac{\gamma}{\lambda_g} \partial_t \lambda_g + \frac{\gamma v_r}{\lambda_g} \partial_r \lambda_g + \frac{1}{T^3} \partial_t (\gamma T^3) + \frac{v_r}{T^3} \partial_r (\gamma T^3) \\ + \gamma \partial_r v_r + \gamma \left(\frac{v_r}{r} + \frac{1}{t} \right) \\ = R_3 (1 - \lambda_g) - 2R_2 \left(1 - \frac{\lambda_q \lambda_{\bar{q}}}{\lambda_g^2} \right), \\ \frac{\gamma}{\lambda_q} \partial_t \lambda_q + \frac{\gamma v_r}{\lambda_q} \partial_r \lambda_q + \frac{1}{T^3} \partial_t (\gamma T^3) + \frac{v_r}{T^3} \partial_r (\gamma T^3) \\ + \gamma \partial_r v_r + \gamma \left(\frac{v_r}{r} + \frac{1}{t} \right) \\ = R_2 \frac{a_1}{b_1} \left(\frac{\lambda_g}{\lambda_q} - \frac{\lambda_{\bar{q}}}{\lambda_g} \right),\end{aligned}\quad (4)$$

where R_2 and R_3 are related to the rates appearing in (3) and are given by,

$$\begin{aligned}R_2 &\approx 0.24 N_f \alpha_s^2 \lambda_g T \ln(1.65/\alpha_s \lambda_g) \\ R_3 &= 1.2 \alpha_s^2 T (2\lambda_g - \lambda_g^2)^{1/2},\end{aligned}\quad (5)$$

v_r is the transverse velocity and $\gamma = 1/\sqrt{1 - v_r^2}$. These will reduce to (34, 35) of Biró et al. [3], if there is no transverse expansion of the system. The hydrodynamic equation (1) is numerically solved to get $\epsilon(r, t)$ and $v_r(r, t)$ which are then used to solve the equations for the fugacities [7]. We have verified that our results near $r = 0$ closely follow the results for a purely longitudinal expansion, till the time when the rarefaction wave has not reached the center. We have solved the hydrodynamic equations by assuming that the initial transverse velocities are zero.

Recall that for a boost invariant longitudinal expansion (1) provides that $\epsilon \tau^{4/3}$ is a constant [9]. Thus in order to bring out the consequences of transverse expansion in a transparent manner, we plot the constant energy density contours $\epsilon(r, t) = \epsilon_i/N^{4/3}$ for $N=1,6,11..,71$ (Figure 1a), which would be lines parallel to the $N=1$ case extending upto $r = R_T$ and separated by $\Delta N t_i$, if there were no transverse expansion of the system. In the present case $N=71$ corresponds to an energy density [10] of 1.45 GeV/fm^3 below which we assume the description in terms of a perturbative QCD plasma to fail. We have also shown a line $r = R_T - c_s t$ which indicates the radial distance of the region affected by the rarefaction wave at any given time t . We see that almost the entire fluid is likely to be affected by the

flow as the life time of the system is sufficiently large. A more rapid cooling of the system is also indicated by the decreasing separation of the contours at later times at, say, $r = 0$. This will affect the evolution of the chemical equilibration in several competing ways.

Thus in Figs. 1b and 1c we show the fugacities for the gluons and the quarks, respectively, along some of the above constant energy density contours. Several interesting observations can be made. We note that the quark fugacities lag behind the gluon fugacities at all times and all radial distances. This is not surprising, considering the lower starting values for λ_q . Recalling that increasing N denotes passage of time, we see that the fugacities at moderate values of r first increase with passage of time. However beyond $N = 31$, ($t \approx 8 \text{ fm}/c$, near $r = 0$) when the transverse expansion of the system is large, it starts decreasing again, except at $r = 0$ where it continues to increase, as all the radial derivatives in (4) are negligible there.

This can be understood by noting that the evolution of the partonic density which is governed by $\partial_\mu(nu^\mu)$ consists of two terms: $u^\mu\partial_\mu n$ which is the rate of change of the density in the comoving frame, and $n\partial_\mu u^\mu$ which is the rate of change of the density due to the expansion of the fluid element in the comoving frame [8]. Once the transverse expansion of the fluid starts developing, the second term and also the radial derivatives in (4) grow very rapidly and drive the system away from chemical equilibrium.

The fugacities decrease monotonically with increase in r which is not surprising because the transverse flow effects grow with increasing r and also the time available to the system in the QGP phase shrinks at larger r . This can have very interesting consequences, the most intriguing of which is the possibility of the formation of a hot and rare partonic system near the surface as compared to a cooler but denser partonic system at the center. Thus, e.g., we estimate that the temperature at the end of our QGP phase is about 200 MeV at $r=6 \text{ fm}$, but only about 160 MeV at $r=0 \text{ fm}$. This variation in the temperature gets more severe at RHIC energies [11], as the life-time of the QGP phase is much smaller there, thus terminating the journey of the partonic system far away from chemical equilibrium. One may create arbitrary competitions between the life-time and the transverse flow effects by considering systems of varying dimensions and initial conditions.

It is not clear whether such a system will go through a mixed phase, say by nucleation of a hadronic droplet [12], at all radial distances even if QCD admits a first order quark-hadron phase transition. Lowering the energy density at which we terminate our calculations will only sharpen this difference as the transverse flow will further enhance the gradients.

The development of the transverse flow and its consequences on the chemical equilibration are sensitively dependent on the evolution of the transverse velocity of the fluid $v_r(r, t)$. In Fig. 2 we have shown the variation of the transverse velocity along some of the constant energy density contours shown in Fig. 1a. We see that the transverse velocity develops rapidly and spreads to smaller radii very quickly, as the speed of sound which drives the pressure is assumed to be rather large. It is conceivable that the speed of sound is reduced when the energy density gets smaller [13]. The life-time of the system would, however, be larger then, and thus the system remains prone to the consequences of the transverse expansion, as seen earlier.

If we now assume that the matter goes to a mixed phase (at small radii, at least), the transverse velocity attained at the end of the QGP phase will stay constant for a comparatively long time, and it may be possible to devise means to actually determine it from the measured particle spectra. Since D-mesons and even B-mesons are expected to be co-

piously produced at LHC energies, the decay leptons from these heavy mesons could serve as indicators of the collective transverse flow, because the leptons will inherit a substantial fraction of the significant kinetic energy carried by their parents. Due to their large mass and relatively small cross sections, the heavy mesons cannot be accelerated to acquire such high velocities in the hadronic phase.

The transverse flow will also affect the spectra of photons and dileptons [14]. We find [11] that the yield of single photons with large transverse momenta increases by a factor of almost 5 due to the transverse expansion, as compared to the situation when there is only a longitudinal expansion. Similar trends are also seen in the transverse mass distribution of dileptons. We have seen that gluon fugacities are larger than the quark fugacities. This provides that the annihilation processes ($\propto \lambda_q \lambda_{\bar{q}}$), give only a small contribution as compared to the Compton processes ($\propto \lambda_g \lambda_q$) to the production of single photons, and can be neglected. Dileptons on the other hand are produced from quark-antiquark annihilation. A comparison of these two measurements could be a valuable source of information on the quark and gluon fugacities of the system [15].

An experimental measurement of the strong transverse flow predicted here would provide two important pieces of evidence about the properties of the dense matter produced in ultrarelativistic heavy ion reactions: that the matter is formed at very high initial pressure, and that this pressure is maintained for a substantial period of time. If the “rarified” partonic matter hadronizes before it attains chemical equilibrium, as is predicted at RHIC energies, it is possible that a mixed phase or a interacting hadronic phase is not created. The emitted hadrons would then reflect the thermal characteristics of the quark phase from which they emerge. We are currently investigating whether another initial parton distribution would lead to a significantly different transverse flow pattern that could be experimentally discriminated from the one predicted here.

Acknowledgments: We acknowledge useful comments from Dr Bikash Sinha. This work was supported in part by a grant from the U.S. Department of Energy (DE-FG02-96ER40945).

REFERENCES

- [1] K. Geiger, Phys. Rep. **258**, 376 (1995).
- [2] K.J. Eskola and X.N. Wang, Phys. Rev. **D49**, 1284 (1994).
- [3] T. S. Biro, E. van Doorn, B. Müller, M. H. Thoma, and X. N. Wang, Phys. Rev. C **48**, 1275 (1993).
- [4] J. Alam, S. Raha, and B. Sinha, Phys. Rev. Lett. **73**, 1895 (1994).
- [5] K. Geiger and J. I. Kapusta, Phys. Rev. D **47**, 4905 (1993).
- [6] K. J. Eskola, B. Müller, and X. N. Wang, Phys. Lett. B **374**, 20 (1996).
- [7] H. von Gersdorff, L. McLerran, M. Kataja, and P. V. Ruuskanen, Phys. Rev. D **34**, 794 (1986).
- [8] K. Kajantie, M. Kataja, and P. V. Ruuskanen, Phys. Lett. B **179**, 153 (1986).
- [9] J. D. Bjorken, Phys. Rev. D **27**, 140 (1983).
- [10] $\epsilon = 1.46 \text{ GeV/fm}^3$ corresponds to the energy density for a fully equilibrated QGP at $T \approx 160 \text{ MeV}$.
- [11] D. K. Srivastava, M. G. Mustafa, and B. Müller, under preparation.
- [12] L.P. Csernai and J.I. Kapusta, Phys. Rev. Lett. **69**, 737 (1992).
- [13] G. Boyd et al., preprint BI-TP 96/04, [\(hep-lat/9602007\)](#).
- [14] B. Kämpfer and O. P. Pavlenko, Z. Phys. C **62**, 491 (1994); Phys. Rev. C **49**, 2716 (1994).
- [15] M. T. Strickland, Phys. Lett. B **331**, 245 (1994).

TABLES

$\tau_i = 0.25 \text{ fm}/c$	RHIC	LHC
$\epsilon_i \text{ (GeV/fm}^3)$	61.4	425
$T_i \text{ (GeV)}$	0.668	1.02
$\lambda_g^{(i)}$	0.34	0.43
$\lambda_q^{(i)}$	0.064	0.082

TABLE I. Initial conditions for the hydrodynamical expansion phase at RHIC and LHC. The initial time is taken as $\tau_i = 0.25 \text{ fm}/c$.

FIGURES

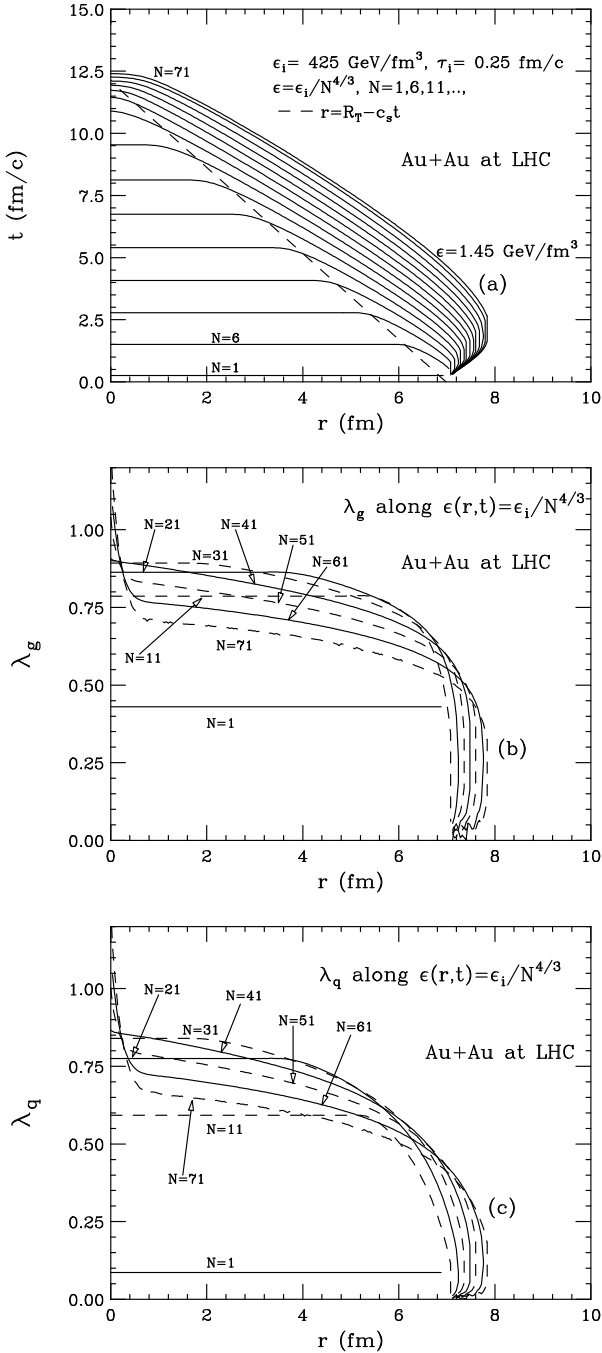


FIG. 1. (a) Constant energy density contours for a transversely expanding quark-gluon plasma likely to be created in Au+Au collisions at LHC. For a boost invariant longitudinal expansion these contours would be equidistant ($\Delta t = 5\tau_i$ at $r = 0$) lines parallel to $N = 1$. The dashed lines give the distance from the axis where the rarefaction wave has arrived at time t , and beyond which the fluid is strongly affected by the flow. (b) Gluon fugacity along some of the constant energy density contours. (c) Quark fugacities along some of the constant energy density density contours.

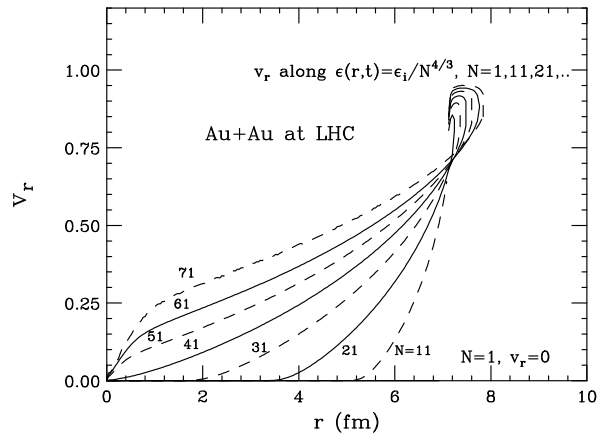


FIG. 2. Transverse velocities along some of the constant energy density contours.